

Collision and recombination driven instabilities in variable charged dusty plasmas

S BAL^{1,2} and M BOSE^{1,*}

¹Department of Physics, Jadavpur University, Kolkata 700 032, India

²Department of AEIE, Dream Institute of Technology, Kolkata, India

*Corresponding author. E-mail: mridulbose@yahoo.co.in

MS received 15 February 2012; accepted 12 October 2012

Abstract. The dust-acoustic instability driven by recombination of electrons and ions on the surface of charged and variably-charged dust grains as well as by collisions in dusty plasmas with significant pressure of background neutrals have been theoretically investigated. The recombination driven instability is shown to be dominant in the long wavelength regime even in the presence of dust-neutral and ion-neutral collisions, while in the shorter wavelength regime, the dust-neutral collision is found to play a major role. In an earlier research work, the dust-neutral collision was neglected in comparison to the effect due to the recombination for estimating the dust-acoustic instability; later the other report shows that the recombination effect is negligible in the presence of dust-neutral collisions. In line of this present situation our investigation revealed that the recombination is more important than dust-neutral collisions in laboratory plasma and fusion plasma, while the dust-neutral collision frequency is dominant in the interstellar plasmas. The effects of ion and dust densities and ion streaming on the recombination and collision driven mode in parameter regimes relevant for many experimental studies on dusty plasmas have also been calculated.

Keywords. Dusty plasma; recombination; dust-neutral collision.

PACS Nos 52.25.Vy; 52.27.Lw; 52.35.–g; 52.35.Fp; 52.35.Qz; 52.20.Hv

1. Introduction

Dusty plasma is loosely defined as normal electron–ion plasma with an additional charged component of micron or submicron-sized particulates. This extra component of macroparticles increases the complexity of the system even further. Dusty plasmas have acquired considerable importance because of their presence in controlled fusion devices [1], astrophysics and planetary physics [2], problems of plasma processing [3], physics of strongly coupled systems [4] etc. Experimentally, one of the important areas of investigation is the study of low-frequency fluctuations in plasma with dust grains. Barkan *et al* [5] has shown that the phase velocity of an ion-acoustic wave increases with the density of negatively charged dust grains and thus ion Landau damping becomes less severe in plasma

with charged dust grains or negative ions [6]. The massive dust grains in the plasma collect electrons and ions from the background plasma thereby acquiring a large electric discharge. The dynamics of these massive particles introduces a variety of new collective wave modes. The study of damping and instability mechanisms associated with such modes has received considerable attention in the context of their possible applications in many space and astrophysical plasmas, plasma processing applications and laboratory plasma experiments.

Major boosts to dusty plasma research occur after numerous experimental and theoretical works on dust-acoustic wave (DAW) [7], the dust ion-acoustic wave (DIAW) [8], the dusty plasma crystal (DPC) [9–11], the lower hybrid drift dissipative wave (LHDDW) [12] and the dust lattice wave (DLW) [13]. A number of laboratory experiments have spectacularly verified the theoretical predictions of the dusty waves [7–12]. One of the collective mode of the dusty plasma, the dust-acoustic mode (DAW), is a low-frequency, low phase velocity longitudinal oscillation, in which the dust particles provide the inertia while Boltzmann distributed electrons and ions provide the thermal pressure effects. The linear dispersion characteristics and instability mechanisms of DAW mode in the presence of free energy sources such as collisions with the background neutrals and ions, equilibrium ion streaming, recombination of ions and electrons on the dust grain surface etc., have also been widely studied [14,15]. Rao *et al* [7] studied theoretically the DAW mode for a fully ionized and collisionless dusty plasma with the assumption of Boltzmann distributed electrons and ions. However, in many experimental conditions, the presence of high neutral pressure and ion streaming can be significant with ion-neutral and dust-neutral mean free paths becoming comparable or shorter than the wavelength of the excited DAW mode [14,16]. In such cases, it is no longer correct to assume a collisionless plasma model with Boltzmann distributed ions and electrons. And, it is important to consider the effects of dust-neutral, ion-neutral collisions and recombination on the dust grain surface of the dust-acoustic mode. D'Angelo and Merlino [17] have investigated the DAW instability in collisional dusty plasma with a significant background neutral pressure and constant DC electric field. Goree *et al* [18] have modelled a stable equilibrium void that results from a balance between the electrostatic and ion drag forces on a dust particle taking into account dust-electron, dust-ion collisions inside the dust region. Kaw and Singh [19] observed collisional instability when dusty plasma was considered with a significant background neutral pressure and with the electron–ion recombination onto the dust grain surface. Mamun and Shukla [20] presented a self-consistent description of low-frequency electrostatic waves and associated damping and instabilities in collisional dusty plasma with the significant background neutrals and ion streaming. Their analysis revealed that in the absence of ion streaming, the dust-acoustic mode is damped due to the combined effects of the collisions and the electron–ion recombination onto the dust surface. The present research effort tries to verify the significance of dust-neutral collision and recombination in contrast with earlier studies [19,20]. Later, Rosenberg [21] investigated ion-dust streaming instability in unmagnetized collisional dusty plasma with frequency less than the dust collision frequency. Under certain conditions, an ion drift in the order of ion thermal speed can excite a resistive instability even when the DAW is heavily damped.

The dust grains in dusty plasma could be either weakly or strongly correlated depending on the strength of the Coulomb coupling parameter $\Gamma = (Z_d e)^2 / a T_d$, where Z_d represents

charge numbers of the dust grain, e is the electronic charge, a is the intergrain distance and T_d is the dust temperature. A dusty plasma can be considered as weakly coupled as long as $\Gamma \ll 1$.

In this study we examine the effects of recombination on the dust surface in the presence of dust-neutral and ion-neutral collisions and ion streaming on the DAW mode in parameter regimes relevant for experimentally studied weakly and strongly coupled dusty plasmas. It is shown that, even in the presence of dust-neutral and ion-neutral collisions, the recombination driven DAW instability is dominant at longer wavelengths. The ion streaming instability is found to be important at shorter wavelength end in the absence of recombination.

This paper is arranged in the following order. In §2, we consider the governing equations for the weakly coupled dusty plasma in the presence of recombination, dust-neutral and ion-neutral collisions. In §3, we derive the linear dispersion relations for the DAW mode for the system due to both weakly coupled regimes under different considerations. The analytical and numerical results for the weakly coupled dusty plasma based on the derived dispersion relation in the absence of ion streaming are presented in §3.1, while §3.2 shows the ion streaming effects on the recombination driven DAW mode for constant dust charge. Section 3.3 shows analytical and numerical results for variable dust charge in the absence of ion streaming. The ion streaming effect on fluctuating charge on dust particles is shown in §3.4. In §4, we have discussed the result and in §5 we have discussed the conclusion.

2. Basic governing equations

In a dusty plasma we consider N_e , N_i , N_d and N_n to be the densities of electrons, ions, the negatively charged dust and neutral gas molecules and T_e , T_i , T_d and T_n to be the respective temperatures. The dust grains are assumed to have spherical shape and to be of the same radius r_d . Ions and dust grains collide with the neutral gas molecules, with collision frequencies ν_{in} , ν_{dn} . The form of ν_{dn} can be obtained by considering the momentum conservation from the force balance equation for the dust and neutral species. As the loss of momentum of one species, due to collisions with the other, has to be gained by the second species, we get $M_n N_n \nu_{nd} \approx M_d N_d \nu_{dn}$. The neutral-dust collisional rate can then be estimated as $\nu_{nd} \approx \pi r_d^2 V_n N_d$. Therefore, the dust-neutral collisional rate is given by $\nu_{dn} \approx (M_n/M_d) N_n \pi r_d^2 V_{td}$ where M_i , M_n and M_d represent masses of ion, neutral and dust particles respectively. We consider unmagnetized uniform dusty plasma consisting of electrons, ions and massive point charged dust particles in the presence of significant background of neutrals. The dust species is assumed to be in the strongly coupled regime and hence we consider dust dynamics modelled through generalized hydrodynamic momentum equation. The basic equations for the dust and ion species are then given by

$$\left[1 + \tau_m \frac{\partial}{\partial t} \right] \left[\frac{\partial V_d}{\partial t} - \frac{Z_d e}{M_d} \nabla \Phi + \frac{\mu_d \gamma_d V_{td}^2}{N_d} \nabla N_d \right] = \eta^* \nabla^2 V_d - \nu_{dn} V_d \quad (1)$$

$$\frac{\partial N_d}{\partial t} + \nabla(N_d V_d) = 0 \quad (2)$$

$$M_i N_i \frac{\partial V_i}{\partial t} = -e N_i \nabla \Phi - T_i \nabla N_i - M_i N_i v_{in} V_i \quad (3)$$

$$\frac{\partial N_i}{\partial t} + \nabla(N_i V_i) = -\nu_R \frac{N_d}{N_{d0}} N_i + S. \quad (4)$$

In the dust momentum eq. (1), τ_m is the relaxation time for the short-range correlations. V_d, Z_d are the velocity and charge of dust particles respectively, while γ_d is the adiabatic index. $V_{td}^2 = T_d/M_d$ is the dust thermal velocity, with dust temperature T_d in energy units and $\mu_d = (1/T_d) (\partial P/\partial N_d)$ is the compressibility and η^* the shear viscosity. Equation (2) is the dust continuity equation. The shear velocity and the dust-neutral collisions provide damping mechanisms for the mode. In the ion momentum eq. (3), V_i, T_i are the ion velocity and temperature (in energy units) respectively, while Φ is the electrostatic wave potential. In the ion continuity eq. (4), $\nu_R = \beta N_{d0} \pi_d^2 c_s$ is the recombination frequency, where $c_s = \sqrt{(T_e/M_i)}$ is the ion-acoustic speed and β is a numerical factor of unity. The term S is the source term accounting for the source of ions produced by the ionization of neutrals by ionizing electrons. The term containing ν_R is the sink term representing the loss of ions due to the recombination of electrons and ions on to the dust grain surface. The form of the recombination rate as defined is obtained from the particle conservation in the ion continuity equation as follows. If $\nu_R N_d$ is the loss rate of ions on to the dust grains, then from species conservation we have $N_i \nu_R = N_d N_i \langle \sigma_R \rangle c_s$ where $\langle \sigma_R \rangle \approx \pi r_d^2$ is the recombination cross-section and it can be seen from here that in equilibrium, the recombination rate $\nu_R = N_d c_s \pi r_d^2$. This recombination rate balances with the ionization rate (S) due to fast ionizing electrons in equilibrium. The electrons are assumed to follow the Boltzmann distribution as the mode frequencies we consider are in the regime $\omega \leq k V_{ti} \leq k V_{te}$. The closure of the system of equations is achieved by the charge neutrality condition, i.e.

$$N_i = N_e + Z_d N_d. \quad (5)$$

3. General dispersion relation

We obtain the linear dispersion relation of electrostatic waves for the system under consideration by carrying out linearization of the above governing equations with normal mode analysis expressing the dependent variables as,

$$N_d = N_{d0} + n_d, \quad V_d = 0 + V_{d1}, \quad N_i = N_{i0} + n_i, \quad V_i = V_{i0} + V_{i1} \quad \text{and} \quad \Phi = \phi_0 + \phi. \quad (6)$$

In the above, the quantities with subscript 0 represent the equilibrium quantities and 1 denotes the first-order-perturbed quantities. In equilibrium, V_{i0} represents the ion streaming velocity and the charge quasineutrality condition $N_{i0} = N_{e0} + Z_d N_{d0}$ is satisfied.

The consideration of inelastic collisions involves extra sink and source terms in continuity equations. In order to calculate the source and the sink terms we start with the continuity equations of ions taking (4)

$$\frac{\partial N_i}{\partial t} + \nabla(N_i V_i) = S - R, \quad (6a)$$

where S and R are the source and the sink terms. The source term $S = \nu_{\text{ion}}N_i$ and sink term is given by $R = \nu_{\text{R}}(N_{\text{d}}/N_{\text{d0}})N_i$.

At equilibrium, sink is equal source,

$$S = R, \quad \nu_{\text{ion}} = \nu_{\text{R}} \left(\frac{N_{\text{d}}}{N_{\text{d0}}} \right).$$

The first-order sink and source term is given by

$$\begin{aligned} \tilde{S} &= \nu_{\text{ion}}\bar{n}_i, \\ \tilde{R} &= \nu_{\text{R}} \left(\frac{n_{\text{d}}}{N_{\text{d0}}} \right) N_i + \nu_{\text{ion}}. \end{aligned}$$

The difference in the source and sink terms takes the form

$$\tilde{S} - \tilde{R} = -\nu_{\text{R}} \left(\frac{n_{\text{d}}}{N_{\text{d0}}} \right) N_i, \quad (6b)$$

where n_{d} is the first-order dust density.

$$\frac{\partial n_i}{\partial t} + V_{i0} \cdot \nabla n_i + N_{i0} \nabla \cdot V_{i1} = (S - R) + (\tilde{S} - \tilde{R}). \quad (6c)$$

The ion continuity equation with first- and zero-order source and sink terms are given by eq. (6c).

The linearized first-order perturbation for dust and ion species equations are given by

$$\left[1 + \tau_m \frac{\partial}{\partial t} \right] \left[\frac{\partial V_{d1}}{\partial t} - \frac{Z_d e}{M_d} \nabla \Phi + \frac{\mu_d \gamma_d V_{td}^2}{N_{d0}} \nabla n_d \right] = \eta^* \nabla^2 V_{d1} - \nu_{\text{dn}} V_{d1}, \quad (7)$$

$$\frac{\partial n_d}{\partial t} + N_{d0} \nabla V_{d1} = 0, \quad (8)$$

$$M_i N_{i0} \frac{\partial V_{i0}}{\partial t} = -e N_{i0} \nabla \Phi - T_i \nabla n_i - M_i N_{i0} \nu_{\text{in}} V_{i1}, \quad (9)$$

$$\frac{\partial n_i}{\partial t} + V_{i0} \cdot \nabla n_i + N_{i0} \nabla \cdot V_{i1} = -\nu_{\text{R}} \frac{N_{i0}}{N_{d0}} n_d, \quad (10)$$

$$n_i = n_e + Z_d n_d. \quad (11)$$

The dust charge fluctuation is governed by Jana *et al* [22].

$$\left(\frac{\partial}{\partial t} + \eta_d \right) q_d = -|I_e| \left(\frac{n_i}{N_{i0}} - \frac{n_e}{N_{e0}} \right) \quad (12)$$

$\eta_d = e |I_e| (T_e^{-1} - \omega_0^{-1})/C$ with $\omega_0 = T_i - e\phi_{f0}$ where ϕ_{f0} is the floating potential on the dust surface, $C \approx r_d$ is the grain capacitance, $|I_e| = (\pi/10) r_d^2 e N_{e0} V_{te}$, $|I_e|$ is the equilibrium current.

The quasineutrality condition for the variable charge is

$$e(n_e - n_i) + N_{d0} q_d + n_d q_{d0} = 0. \quad (13)$$

$q_d = eZ_d$ where Z_d is the equilibrium charge number on the surface of the dust grains. We now consider Fourier transformation of the above equations assuming all perturbed

quantities to vary as proportional to $\exp(i(kx - \omega t))$. We obtain the linear dispersion relation, where ω is the angular frequency and k is the wave number, from the basic equations.

The continuity equation for dust particles, i.e. eq. (8), gives

$$\tilde{n}_d = \frac{kV_{d1}}{\omega}. \quad (14)$$

Here, we denote $\tilde{n}_d = n_d/N_{d0}$. From the dust momentum eq. (7) we write

$$\begin{aligned} & [\omega(1 - \omega\tau_m) + iv_{dn} + i\eta^*k^2]V_{d1} \\ & = -[1 - i\omega\tau_m]kc_D^2\tilde{\phi} + [1 - i\omega\tau_m]kV_{id}^2\mu_d\gamma_d\tilde{n}_d, \end{aligned} \quad (15)$$

where $\tilde{\phi} = e\phi/T_e$. From the Boltzmann distribution for electrons, we obtain, for the perturbed electron density

$$\tilde{n}_e = \tilde{\phi}. \quad (16)$$

In the ion momentum eq. (9), we assume that $v_{in} \geq \partial V_i/\partial t$ and consequently the RHS of (9) is zero. Therefore we write,

$$V_{i1} = \frac{-ikV_{ii}^2}{v_{in}} [\tau\tilde{\phi} + \tilde{n}_i], \quad (17)$$

where we have defined $\tau = T_e/T_i$ and $\tilde{n}_i = n_i/N_{i0}$. From the linearized ion continuity eq. (10) we get

$$[-i(\omega - kV_{i0})]\tilde{n}_i + ikV_{i1} = -\nu_R\tilde{n}_d. \quad (18)$$

Making use of (11), (14), (15), (17) and (18), we obtain the following dispersion relation:

$$\begin{aligned} & \left[1 - \frac{k^2c_D^2(1 - i\omega\tau_m)}{[\omega(\omega + iv_{dn}) + i\omega\eta^*k^2 - i\omega^3\tau_m - k^2V_{id}^2\mu_d\gamma_d(1 - i\omega\tau_m)]} \right] \\ & \times \left[1 - \frac{iv_{in}}{k^2V_{ii}^2}(\omega - kV_{i0}) \right] \\ & + \tau_* - \left[\frac{\alpha\nu_Rv_{in}(1 - i\omega\tau_m)}{[\omega(\omega + iv_{dn}) + i\omega\eta^*k^2 - i\omega^3\tau_m - k^2V_{id}^2\mu_d\gamma_d(1 - i\omega\tau_m)]} \right] = 0. \end{aligned} \quad (19)$$

Equation (19) is the linear dispersion relation for dust-acoustic waves in an unmagnetized dusty plasma system taking into account the strong coupling effects, ion-neutral and dust-neutral collisions and recombination of ions and electrons on the surface of dust grains. In this relation we have defined $c_{D*}^2 = c_D^2Z_dN_{d0}/N_{e0}$, with $c_D^2 = Z_dT_e/M_d$ being the dust-acoustic velocity, $\alpha = c_D^2N_{i0}/V_{ii}^2N_{e0}$ and $\tau_* = T_eN_{i0}/T_iN_{e0}$. The strong coupling effects of the dust grains enter through the terms τ_m , μ_d and damping term-shear viscosity η^* . We can consider solutions of the dispersion relation in the limits $\omega\tau_m \ll 1$ called the hydrodynamic modes and in the opposite limit $\omega\tau_m \gg 1$ called the kinetic modes. The corresponding dispersion relation for the weakly coupled plasmas ($\Gamma \ll 1$) can be

obtained from (17) by setting τ_m, μ_d and η^* equal to zero. Therefore, the weak coupled limit of the dispersion relation is given by

$$\begin{aligned} & [(\omega^2 + i\omega\nu_{dn}) - k^2 c_{D^*}^2] \left[1 - \frac{i\nu_{in}}{k^2 V_{i0}^2} (\omega - kV_{i0}) \right] \\ & + [(\omega^2 + i\omega\nu_{dn}) \tau_* - \alpha\nu_R \nu_{in}] = 0. \end{aligned} \quad (20)$$

The dispersion relation for variable charged dust particles using eqs (12)–(18)

$$\begin{aligned} & \{(\omega^2 + i\omega\nu_{dn}) [\omega + i(\eta_d + I_0b)] - k^2 C_{D^*}^2 (\omega^2 + i\eta_d)\} \\ & \times \left\{ 1 - i \frac{\nu_{in}}{k^2 V_{i0}^2} (\omega - kV_{i0}) \right\} \\ & + \left\{ [\omega + i(\eta_d + I_0a)] [(\omega^2 + i\omega\nu_{dn}) \tau_* - \alpha\nu_R \nu_{in}] \right\} = 0 \end{aligned} \quad (21)$$

$$A = \nu_{dn}(\eta_d + I_0b) + \nu_{dn}(\eta_d + I_0a)\tau_* + k^2 C_{D^*}^2 \left(1 + \frac{\eta_d \nu_{in}}{k^2 V_{i0}^2} \right) + \alpha\nu_R \nu_{in}$$

$$B = 1 + \tau_* + \frac{\nu_{in}}{k^2 V_{i0}^2} (\nu_{dn} + \eta_d + I_0b)$$

$$C = \nu_{dn}(1 + \tau_*) + (\eta_d + I_0b) \left(1 + \frac{\nu_{dn} \nu_{in}}{k^2 V_{i0}^2} \right) + \frac{k^2 C_{D^*}^2 \nu_{in}}{k^2 V_{i0}^2} + (\eta_d + I_0a)\tau_*$$

$$D = (\eta_d + I_0a) \alpha\nu_R \nu_{in} + k^2 C_{D^*}^2 \eta_d$$

$$I_0 = \frac{|I_e|}{eZ_{d0}}, \quad a = \frac{Z_{d0}N_{d0}}{N_{i0}}, \quad b = \frac{Z_{d0}N_{d0}}{N_{e0}}.$$

3.1 Dispersion properties with dust-neutral collision, as well as recombination effects when ions are initially at rest ($\nu_{dn} \neq 0, \nu_R \neq 0$ and $V_{i0} = 0$) for constant charge

In this section we first consider the dispersion properties of the mode without the ion streaming ($V_{i0} = 0$) for a weakly coupled dusty plasma and obtain an analytical solution. A numerical investigation of the dispersion relation is then presented for parameters relevant to experimental conditions. We solve the above dispersion relation (20) for complex $\omega = \omega_r + i\gamma$ with $\gamma \leq \omega_r$ to obtain the real frequency and growth rate as

$$\omega_r^2 = \frac{k^2 c_{D^*}^2 (1 + (\nu_{in} \nu_R / k^2 V_{i0}^2)) + \alpha\nu_R \nu_{in}}{1 + \tau_* + (\nu_{in} \nu_{dn} / k^2 V_{i0}^2)} \quad (22)$$

$$\gamma = \frac{(\nu_{in} / k^2 V_{i0}^2) (\omega_r^2 - k^2 C_{D^*}^2) - \nu_{dn} (1 + \tau_*)}{2 \left[1 + \tau_* + (\nu_{in} \nu_{dn} / k^2 V_{i0}^2) \right]}. \quad (23)$$

Next, considering $\alpha\nu_{in} \nu_R \ll k^2 c_{D^*}^2$ we can rewrite γ from eq. (20) as

$$\gamma \approx \frac{\nu_{in}}{2(1 + \tau_*)^2} \left[\frac{\alpha\nu_{in} \nu_R (1 + \tau_*)}{k^2 V_{i0}^2} - \tau_* \frac{c_{D^*}^2}{V_{i0}^2} \right] - \frac{\nu_{dn}}{2}. \quad (24)$$

Here, we see from eq. (21) that the excited wave will grow when $\alpha\nu_R > \tau_* [c_{D^*}^2 / \nu_{in} (1 + \tau_*)]$.

3.2 Dispersion properties with dust-neutral collision, recombination and ion streaming ($v_{dn} \neq 0$, $v_R \neq 0$ and $V_{i0} \neq 0$) for constant charge

An instability driven by recombination can occur only at longer wavelengths. However, if we include ion drift in this range of wavelengths, it is easy to see that it reduces the recombination instability growth rates. For finite V_{i0} , ion drift driven instability is possible when $V_{i0} > \omega_r/k$ and $\alpha v_R < \tau_* [c_{D^*}^2/v_{in}(1 + \tau_*)]$. For a complete study of the effects of dust-neutral, ion-neutral and recombination on the wave mode in the presence of ion streaming, we now consider the numerical analysis of the dispersion relation (20) to obtain the real frequency as well as growth rate, as shown below:

$$\omega_r = \frac{\left\{ \begin{array}{l} (v_{in}v_{dn}kV_{i0}/k^2V_{ii}^2) \pm \sqrt{(v_{in}v_{dn}kV_{i0}/k^2V_{ii}^2)^2} \\ -4 \left[1 + \tau_* + (v_{in}v_{dn}/k^2V_{ii}^2) \{ -k^2C_{D^*}^2 - \alpha v_R v_{in} \} \right] \end{array} \right\}}{2 \left[1 + \tau_* + (v_{in}v_{dn}/k^2V_{ii}^2) \right]} \quad (25)$$

$$\gamma = \frac{[(\omega_r - kV_{i0})v_{in}/k^2V_{ii}^2] \{ \omega_r^2 - k^2C_{D^*}^2 \} - \omega_r v_{dn} \{ 1 + \tau_* \}}{2\omega_r \left[1 + \tau_* + (v_{in}v_{dn}/k^2V_{ii}^2) \right] - (v_{dn}v_{in}kV_{i0}/k^2V_{ii}^2)}. \quad (26)$$

3.3 Dispersion properties with dust-neutral collision, as well as recombination effects when ions are initially at rest ($v_{dn} \neq 0$, $v_R \neq 0$ and $V_{i0} = 0$) for variable charge

The dispersion relation for weakly coupled dusty plasma with variable charge is given by eq. (21). In order to solve the real frequency and growth rate of the excited wave in the absence of ion streaming, we separate the real and imaginary parts of the dispersion relation (21) by substituting $\omega = \omega_r + i\gamma$ where ω_r and γ represent real frequency and growth rate of the low-frequency wave given by

$$\omega_r^2 = \frac{(v_{dn}(\eta_d + I_0b) + v_{dn}(\eta_d + I_0a)\tau_* + k^2C_{D^*}^2(1 + (\eta_d v_{in}/k^2V_{ii}^2)) + \alpha v_R v_{in})}{(1 + \tau_* + (v_{in}/k^2V_{ii}^2)(v_{dn} + \eta_d + I_0b))} \quad (27)$$

$$\gamma = \frac{(v_{in}/k^2V_{ii}^2)\omega_{rvar}^4 - C\omega_{rvar}^2 + D}{3\omega_{rvar}^2 B - A} \quad (28)$$

where

$$I_0 = \frac{|I_e|}{eZ_{d0}}, \quad a = \frac{Z_{d0}N_{d0}}{N_{i0}}, \quad b = \frac{Z_{d0}N_{d0}}{N_{e0}},$$

$$A = v_{dn}(\eta_d + I_0b) + v_{dn}(\eta_d + I_0a)\tau_* + k^2C_{D^*}^2 \left(1 + \frac{\eta_d v_{in}}{k^2V_{ii}^2} \right) + \alpha v_R v_{in},$$

$$B = 1 + \tau_* + \frac{v_{in}}{k^2V_{ii}^2} (v_{dn} + \eta_d + I_0b),$$

$$D = (\eta_d + I_0a) \alpha v_R v_{in} + k^2C_{D^*}^2 \eta_d.$$

3.4 Dispersion properties with dust-neutral collision, recombination and ion streaming ($v_{dn} \neq 0$, $v_R \neq 0$ and $V_{i0} \neq 0$) for variable charge

In the presence of ion streaming, we consider (21) and isolate the real and imaginary parts from the dispersion relation for variable in weakly coupled dusty plasma. The real part of (21) in the presence of ion streaming is $D_r(\omega)$, given by (29).

$$\begin{aligned}
 D_r(\omega) = & \omega^3 \left(1 + \frac{v_{in}}{k^2 V_{ti}^2} (v_{dn} + \eta_d + I_0 b) + \tau_* \right) \\
 & - \omega^2 \left[\frac{v_{in} k V_{i0}}{k^2 V_{ti}^2} (v_{dn} + \eta_d + I_0 b) \right] \\
 & - \omega \left[v_{dn} (\eta_d + I_0 b) + v_{dn} (\eta_d + I_0 a) \tau_* \right. \\
 & \left. + k^2 C_{D^*}^2 \left(1 + \frac{\eta_d v_{in}}{k^2 V_{ti}^2} \right) + \alpha v_R v_{in} \right] + \frac{k^2 C_{D^*}^2 \eta_d v_{in} k V_{i0}}{k^2 V_{ti}^2}. \quad (29)
 \end{aligned}$$

Solving $D_r(\omega) = 0$ at $V_{i0} \neq 0$ we solve numerically the value of real frequency. The growth rate may be evaluated numerically by solving $(\gamma = -D_i(\omega)/(\partial D_r/\partial \omega_r))$ at $V_{i0} \neq 0$ where

$$\begin{aligned}
 \frac{\partial D_r}{\partial \omega_r} = & 3\omega_r^2 \text{var} \left(1 + \frac{v_{in}}{k^2 V_{ti}^2} (v_{dn} + \eta_d + I_0 b) + \tau_* \right) \\
 & - 2\omega_r \text{var} \left(\frac{v_{in} k V_{i0}}{k^2 V_{ti}^2} (v_{dn} + \eta_d + I_0 b) \right) \\
 & - v_{dn} (\eta_d + I_0 b) + v_{dn} (\eta_d + I_0 a) \tau_* + k^2 C_{D^*}^2 \left(1 + \frac{\eta_d v_{in}}{k^2 V_{ti}^2} \right) \\
 & + \alpha v_R v_{in}, \quad (30)
 \end{aligned}$$

$$\begin{aligned}
 D_i(\omega) = & \omega^4 \left(\frac{-v_{in}}{k^2 V_{ti}^2} \right) + \omega^3 \left(\frac{v_{in} k V_{i0}}{k^2 V_{ti}^2} \right) \\
 & + \omega^2 \left[v_{dn} (1 + \tau_*) + (\eta_d + I_0 b) \left(1 + \frac{v_{dn} v_{in}}{k^2 V_{ti}^2} \right) \right. \\
 & \left. + \frac{k^2 C_{D^*}^2 v_{in}}{k^2 V_{ti}^2} + (\eta_d + I_0 a) \tau_* \right] \\
 & - \omega \left[\frac{v_{dn} (\eta_d + I_0 b) v_{in} k V_{i0}}{k^2 V_{ti}^2} + \frac{k^2 C_{D^*}^2 v_{in} k V_{i0}}{k^2 V_{ti}^2} \right] \\
 & - [(\eta_d + I_0 a) \alpha v_R v_{in} + k^2 C_{D^*}^2 \eta_d]. \quad (31)
 \end{aligned}$$

We numerically solve eq. (21) for variable charge and obtain the real frequency and growth rates for different V_{i0} . For numerical solutions of eqs (21) and (22)–(31) we choose the parameters of the experiments of Prabhuram and Goree [16] as, $M_i = 12M_p$, where M_p is the mass of proton, $M_d = 2.4 \times 10^8 M_p$, $N_{i0} = 5 \times 10^{10} \text{ cm}^{-3}$, $N_{d0} = 1 \times 10^7 \text{ cm}^{-3}$, $Z_d = 200$, $T_e = 0.4 \text{ eV}$, $T_i = 0.1 \text{ eV}$, $T_d = 300 \text{ K}$, $r_d = 50 \text{ nm}$, $\beta = 1$, $\sigma_{in} = 1 \times 10^{-14} \text{ cm}^2$, $N_n = 1 \times 10^{16} - 1 \times 10^{17} \text{ cm}^{-3}$ and $V_{i0} = 0 - 5V_{te}$.

4. Discussion

4.1 At initially immobile ions, i.e. $V_{i0} = 0$

4.1.1 *Neutral density effects.* The combined effects of dust-neutral and ion-neutral collisions in the presence of recombination on the dust grain surface are shown in figures 1 and 2. In figure 1, we have plotted the real frequency (ω_r) of the dust-acoustic mode for the above given parameters [16] as a function of the wave vector k for various neutral densities, $N_n = 1 \times 10^{16}, 2 \times 10^{16}, 3 \times 10^{16}, 5 \times 10^{16}$ and $1 \times 10^{17} \text{ cm}^{-3}$. The corresponding growth rates (γ) shown in figure 2 shows similar nature of [19] as well as [20] while considering both dust-neutral and ion-neutral collisions in the presence of recombination on the dust grain surface. While attempting this problem, Kaw and Singh [19] and Mamun and Shukla [20] have considered the dominance of only one type of damping mechanism while in our case we have considered both the damping mechanism and showed that the

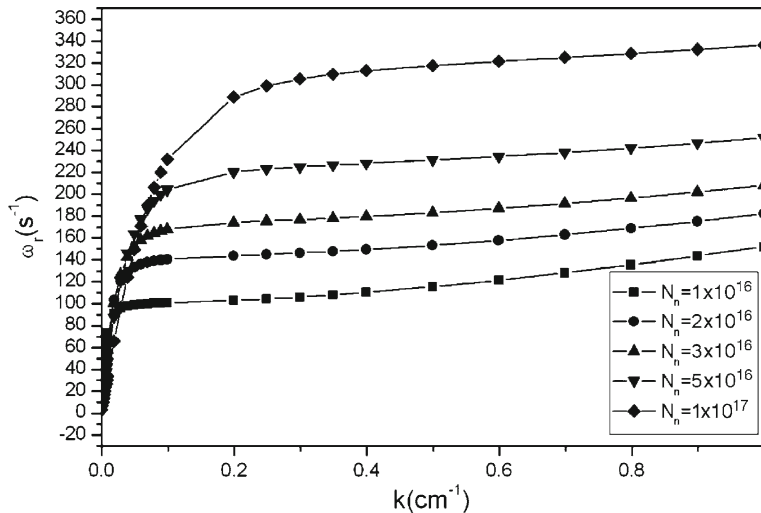


Figure 1. Real frequency ω_r vs. k , for constant charge, with $V_{i0} = 0$, for different neutral number densities $N_n = 1 \times 10^{16} \text{ cm}^{-3}, 2 \times 10^{16} \text{ cm}^{-3}, 3 \times 10^{16} \text{ cm}^{-3}, 5 \times 10^{16} \text{ cm}^{-3}, 1 \times 10^{17} \text{ cm}^{-3}$.

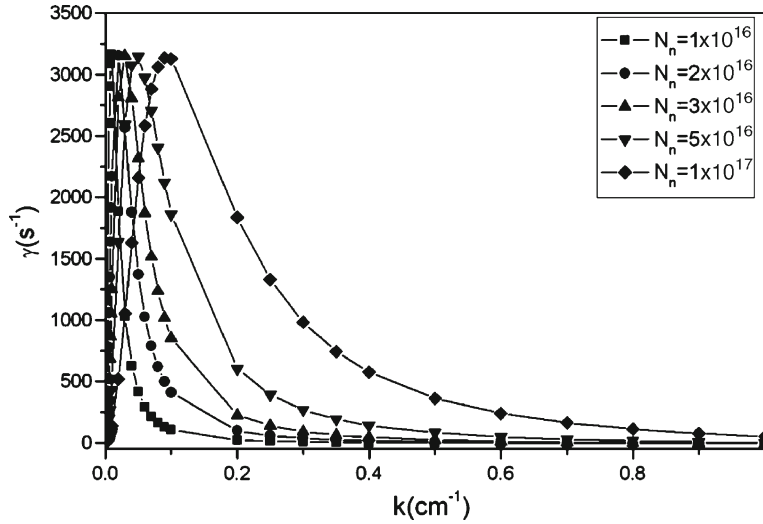


Figure 2. Growth rate γ vs. k , for constant charge, with $V_{i0} = 0$, for different neutral number densities $N_n = 1 \times 10^{16} \text{ cm}^{-3}$, $2 \times 10^{16} \text{ cm}^{-3}$, $3 \times 10^{16} \text{ cm}^{-3}$, $5 \times 10^{16} \text{ cm}^{-3}$, $1 \times 10^{17} \text{ cm}^{-3}$.

excited wave will grow with time in contrast to the result reported in [20]. The study of variable dust charge as shown in figures 3 and 4 respectively represents the variation of real frequency (ω_r) and growth rates (γ) as a function of wave vector k for various

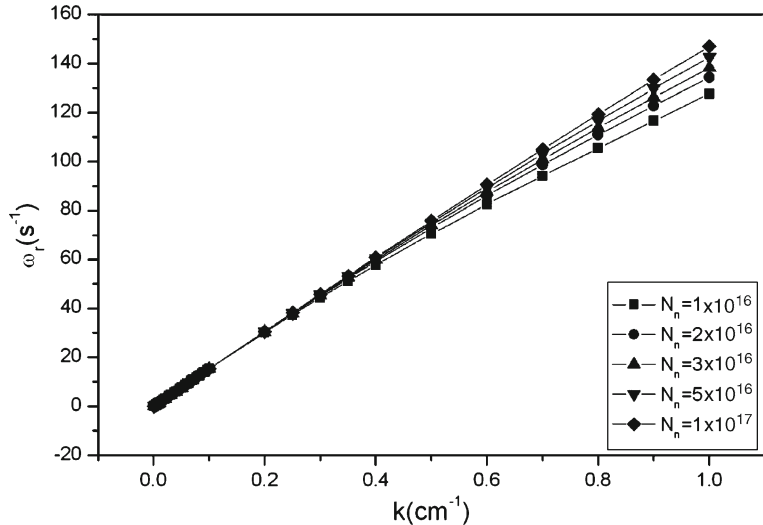


Figure 3. Real frequency ω_r vs. k , for fluctuating dust charge with $V_{i0} = 0$, for different neutral number densities $N_n = 1 \times 10^{16} \text{ cm}^{-3}$, $2 \times 10^{16} \text{ cm}^{-3}$, $3 \times 10^{16} \text{ cm}^{-3}$, $5 \times 10^{16} \text{ cm}^{-3}$, $1 \times 10^{17} \text{ cm}^{-3}$.

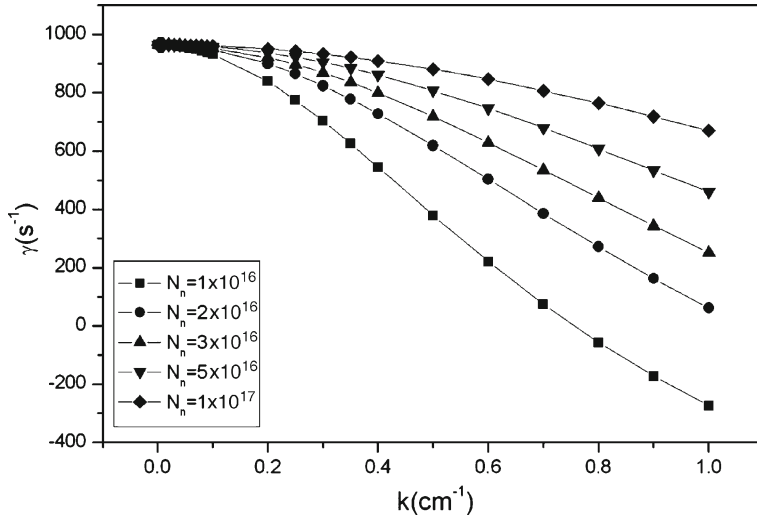


Figure 4. Growth rate γ vs. k , for variable dust charge with $V_{i0} = 0$, for different neutral number densities $N_n = 1 \times 10^{16} \text{ cm}^{-3}$, $2 \times 10^{16} \text{ cm}^{-3}$, $3 \times 10^{16} \text{ cm}^{-3}$, $5 \times 10^{16} \text{ cm}^{-3}$, $1 \times 10^{17} \text{ cm}^{-3}$.

neutral densities at $V_{i0} = 0$. In both constant and fluctuating dust charge variations, we find positive growth rates at $V_{i0} = 0$, but in variable dust charge, damping of growth rates or negative growth rates exist as shown in figure 4.

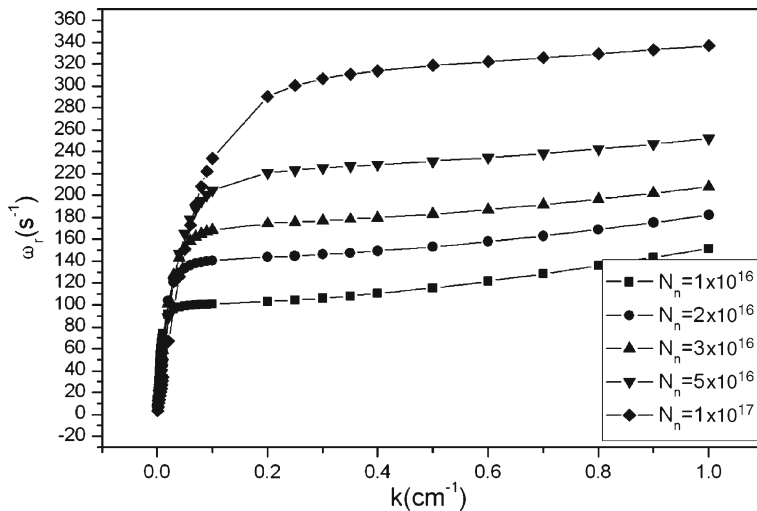


Figure 5. Real frequency ω_r vs. k , for constant charge, with $V_{i0} = 0.001 V_{i1}$, for different neutral number densities $N_n = 1 \times 10^{16} \text{ cm}^{-3}$, $2 \times 10^{16} \text{ cm}^{-3}$, $3 \times 10^{16} \text{ cm}^{-3}$, $5 \times 10^{16} \text{ cm}^{-3}$, $1 \times 10^{17} \text{ cm}^{-3}$.

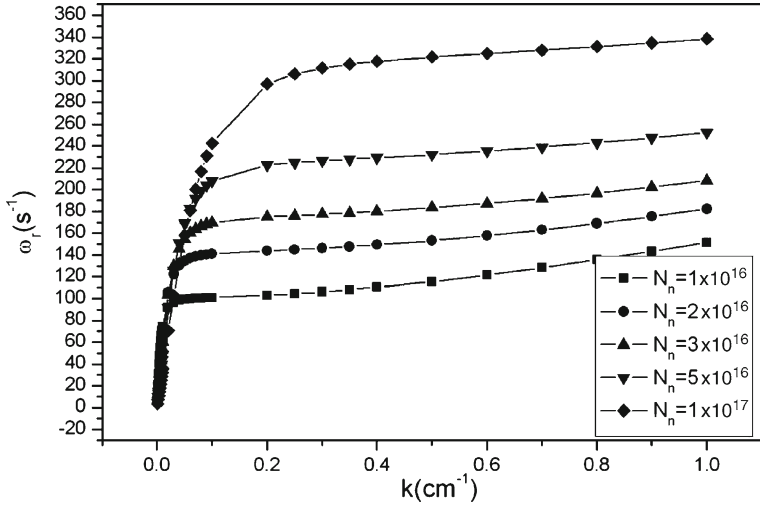


Figure 6. Real frequency ω_r vs. k , for constant charge, with $V_{i0} = 0.005V_{ii}$, for different neutral number densities $N_n = 1 \times 10^{16} \text{ cm}^{-3}$, $2 \times 10^{16} \text{ cm}^{-3}$, $3 \times 10^{16} \text{ cm}^{-3}$, $5 \times 10^{16} \text{ cm}^{-3}$, $1 \times 10^{17} \text{ cm}^{-3}$.

4.2 In the presence of ion streaming, i.e. $V_{i0} \neq 0$

4.2.1 *Neutral density effects.* We consider the effects of streaming velocity in the presence of dust-neutral collisions as well as recombination on the dust grain surface.

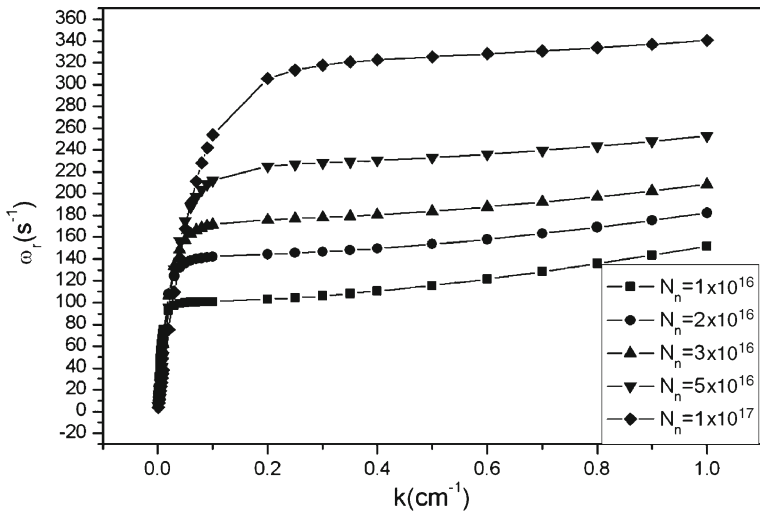


Figure 7. Real frequency ω_r vs. k , for constant charge, with $V_{i0} = 0.01 V_{ii}$, for different neutral number densities $N_n = 1 \times 10^{16} \text{ cm}^{-3}$, $2 \times 10^{16} \text{ cm}^{-3}$, $3 \times 10^{16} \text{ cm}^{-3}$, $5 \times 10^{16} \text{ cm}^{-3}$, $1 \times 10^{17} \text{ cm}^{-3}$.

Figures 5–7 represent the real frequency (ω_r) as a function of wave vector k of the dust-acoustic mode, for various neutral densities, at $V_{i0} = 0.001V_{ti}$, $0.005V_{ti}$ and $0.01V_{ti}$ respectively. Here we find two growth rates for each V_{i0} from eqs (22) and (23). The growth rates for different $V_{i0} = 0.001V_{ti}$, $0.005V_{ti}$ and $0.01V_{ti}$ are shown in figures 8a–b, 9a–b and 10a–b respectively. When dust charge fluctuation is considered

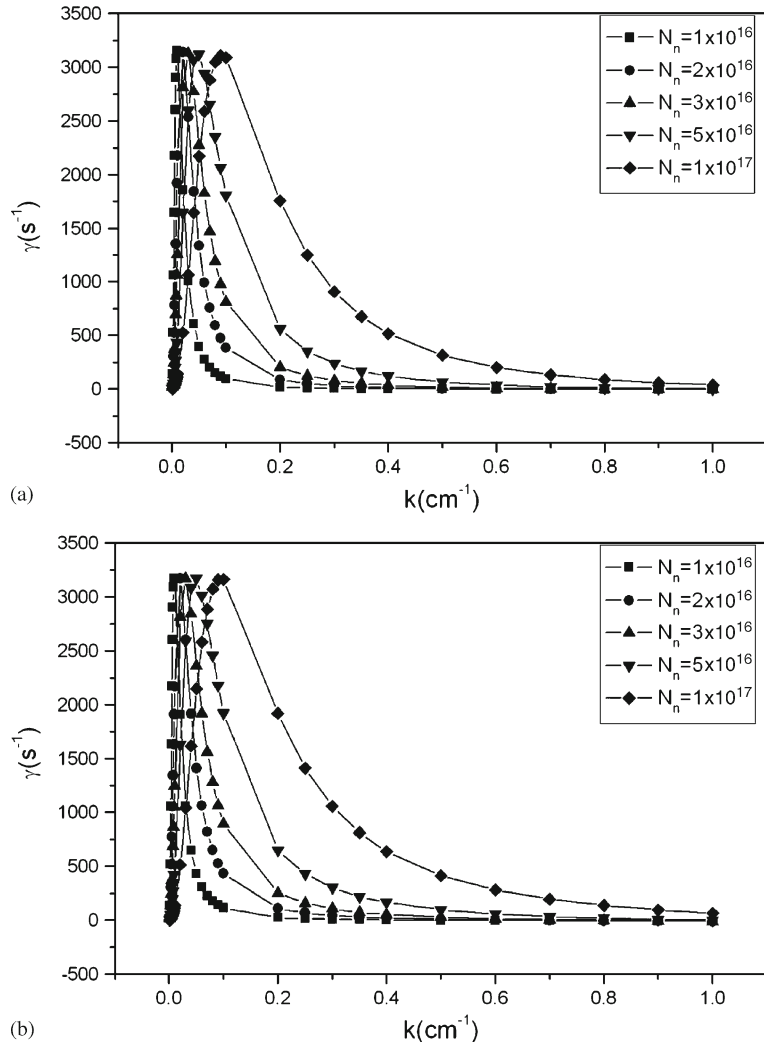
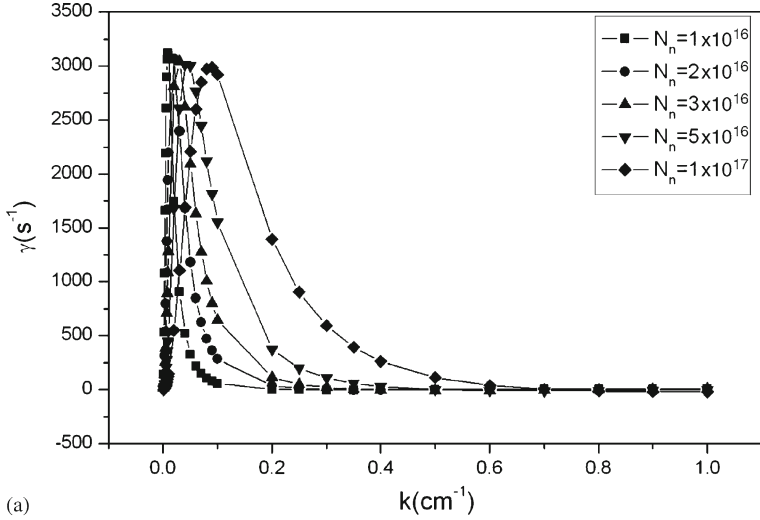
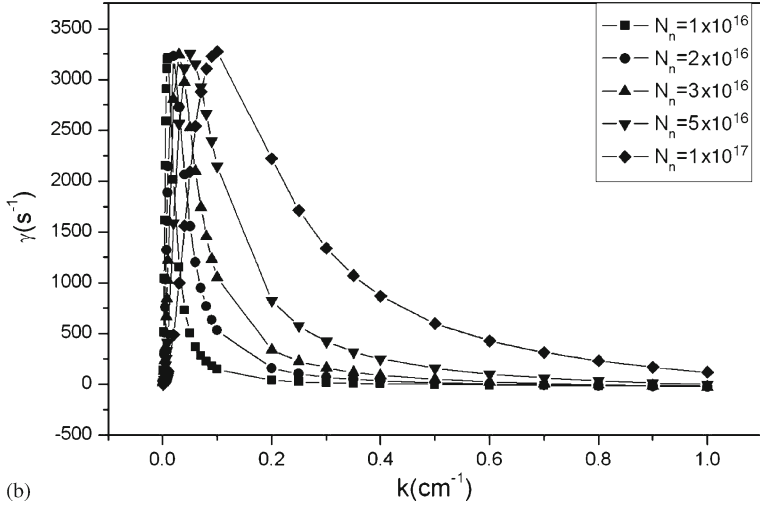


Figure 8. (a) The first growth rate γ vs. k , for constant charge, with $V_{i0} = 0.001V_{ti}$, for different neutral number densities $N_n = 1 \times 10^{16} \text{ cm}^{-3}$, $2 \times 10^{16} \text{ cm}^{-3}$, $3 \times 10^{16} \text{ cm}^{-3}$, $5 \times 10^{16} \text{ cm}^{-3}$, $1 \times 10^{17} \text{ cm}^{-3}$. (b) The second growth rate γ vs. k , for constant charge, with $V_{i0} = 0.001V_{ti}$, for different neutral number densities $N_n = 1 \times 10^{16} \text{ cm}^{-3}$, $2 \times 10^{16} \text{ cm}^{-3}$, $3 \times 10^{16} \text{ cm}^{-3}$, $5 \times 10^{16} \text{ cm}^{-3}$, $1 \times 10^{17} \text{ cm}^{-3}$.



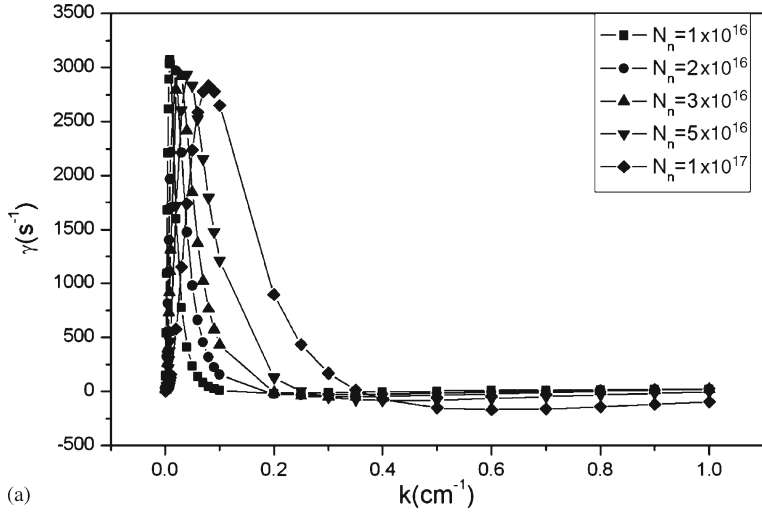
(a)



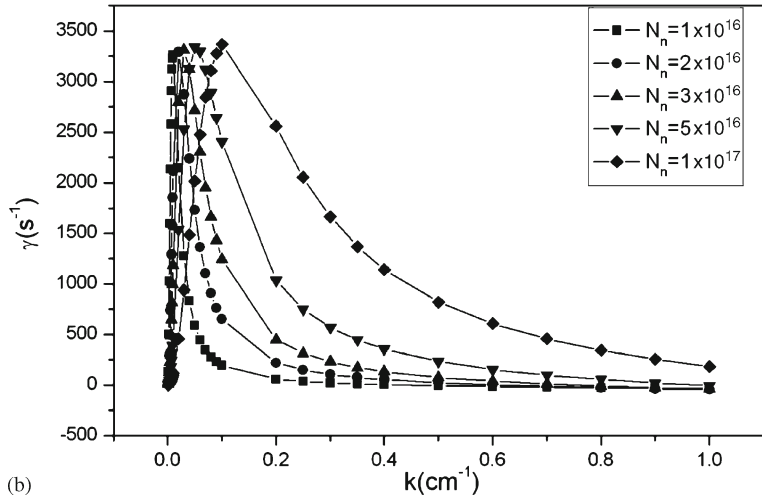
(b)

Figure 9. (a) The first growth rate γ vs. k , for constant charge, with $V_{i0} = 0.005 V_{ti}$, for different neutral number densities $N_n = 1 \times 10^{16} \text{ cm}^{-3}$, $2 \times 10^{16} \text{ cm}^{-3}$, $3 \times 10^{16} \text{ cm}^{-3}$, $5 \times 10^{16} \text{ cm}^{-3}$, $1 \times 10^{17} \text{ cm}^{-3}$. (b) The second growth rate γ vs. k , for constant charge, with $V_{i0} = 0.005 V_{ti}$, for different neutral number densities $N_n = 1 \times 10^{16} \text{ cm}^{-3}$, $2 \times 10^{16} \text{ cm}^{-3}$, $3 \times 10^{16} \text{ cm}^{-3}$, $5 \times 10^{16} \text{ cm}^{-3}$, $1 \times 10^{17} \text{ cm}^{-3}$.

we have real frequency and growth rates as a function of wave vector k for various neutral densities at $V_{i0} = 0.001 V_{ti}$, $0.005 V_{ti}$ and $0.01 V_{ti}$ as shown in figures 11, 12 and 13 respectively. The corresponding growth rates at $V_{i0} = 0.001 V_{ti}$, $0.005 V_{ti}$ and $0.01 V_{ti}$ as shown in figures 14, 15 and 16 respectively.



(a)



(b)

Figure 10. (a) The first growth rate γ vs. k , for constant charge, with $V_{i0} = 0.01V_{ti}$, for different neutral number densities $N_n = 1 \times 10^{16} \text{ cm}^{-3}$, $2 \times 10^{16} \text{ cm}^{-3}$, $3 \times 10^{16} \text{ cm}^{-3}$, $5 \times 10^{16} \text{ cm}^{-3}$, $1 \times 10^{17} \text{ cm}^{-3}$. (b) The second growth rate γ vs. k , for constant charge, with $V_{i0} = 0.01V_{ti}$, for different neutral number densities $N_n = 1 \times 10^{16} \text{ cm}^{-3}$, $2 \times 10^{16} \text{ cm}^{-3}$, $3 \times 10^{16} \text{ cm}^{-3}$, $5 \times 10^{16} \text{ cm}^{-3}$, $1 \times 10^{17} \text{ cm}^{-3}$.

4.3 Validity regime for dust-neutral collision and recombination driven instabilities

Competition between dust-neutral collisions and recombination driven instabilities are shown in figures 17a–b where we found that the recombination driven instability is more active than the dust-neutral collision instability in the long wavelength regime whereas

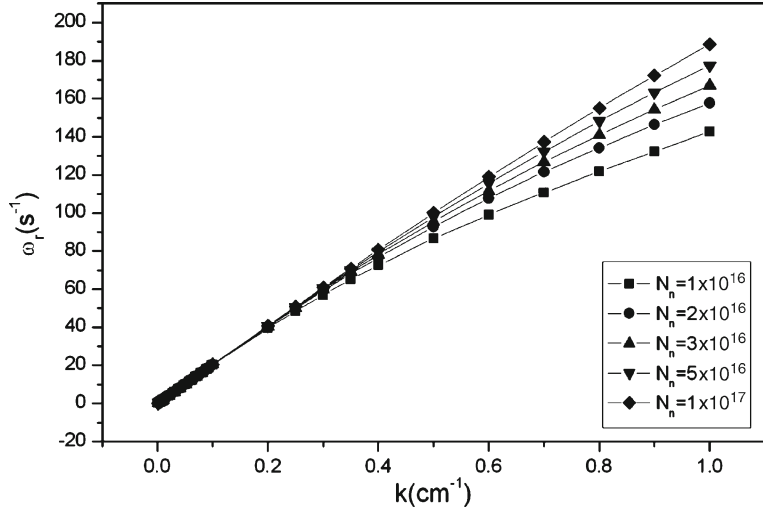


Figure 11. Real frequency ω_r vs. k , of variable dust charge with $V_{i0} = 0.001V_{ii}$, for different neutral number densities $N_n = 1 \times 10^{16} \text{ cm}^{-3}$, $2 \times 10^{16} \text{ cm}^{-3}$, $3 \times 10^{16} \text{ cm}^{-3}$, $5 \times 10^{16} \text{ cm}^{-3}$, $1 \times 10^{17} \text{ cm}^{-3}$.

in short wavelength regime the latter becomes the important contributor. This result is contrary to the result obtained by Mamun and Shukla [20] where they have reported that the recombination effect is negligible in the presence of dust-neutral collision. But

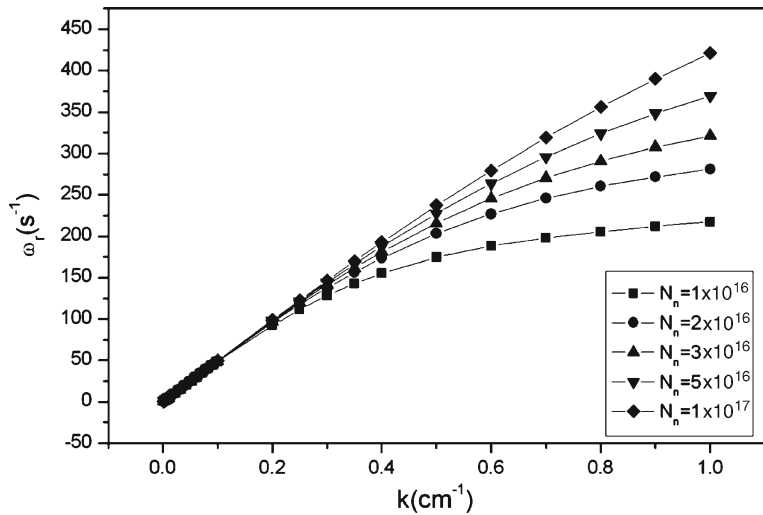


Figure 12. Real frequency ω_r vs. k , of variable dust charge with $V_{i0} = 0.005V_{ii}$, for different neutral number densities $N_n = 1 \times 10^{16} \text{ cm}^{-3}$, $2 \times 10^{16} \text{ cm}^{-3}$, $3 \times 10^{16} \text{ cm}^{-3}$, $5 \times 10^{16} \text{ cm}^{-3}$, $1 \times 10^{17} \text{ cm}^{-3}$.

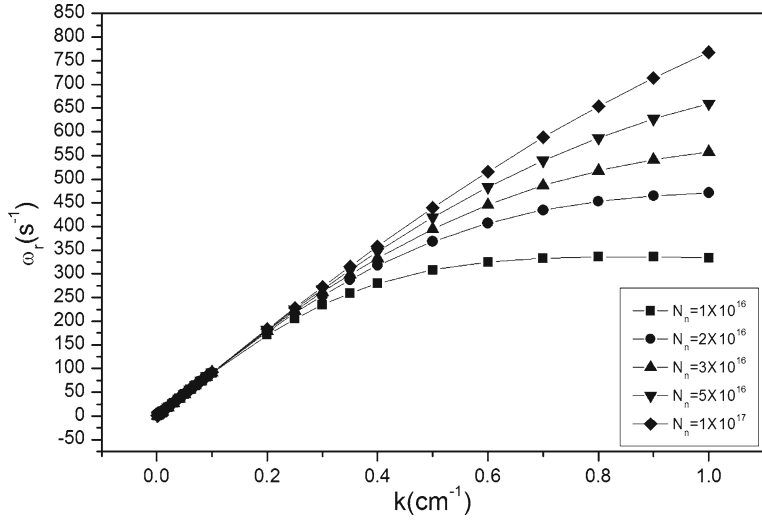


Figure 13. Real frequency ω_r vs. k , of variable dust charge with $V_{i0} = 0.01V_{ti}$, for different neutral number densities $N_n = 1 \times 10^{16} \text{ cm}^{-3}$, $2 \times 10^{16} \text{ cm}^{-3}$, $3 \times 10^{16} \text{ cm}^{-3}$, $5 \times 10^{16} \text{ cm}^{-3}$, $1 \times 10^{17} \text{ cm}^{-3}$.

in the earlier paper, Kaw and Singh [19] have neglected the dust-neutral collisions in comparison to the effect due to recombination for estimating the damping mechanisms in a dusty plasma. We then calculated both the damping factors with the help of the given

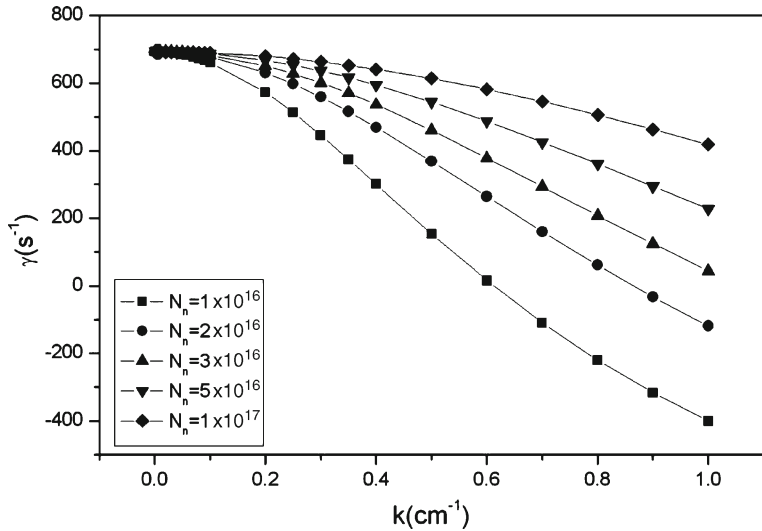


Figure 14. Growth rate γ vs. k , of variable charge with $V_{i0} = 0.001V_{ti}$, for different neutral number densities $N_n = 1 \times 10^{16} \text{ cm}^{-3}$, $2 \times 10^{16} \text{ cm}^{-3}$, $3 \times 10^{16} \text{ cm}^{-3}$, $5 \times 10^{16} \text{ cm}^{-3}$, $1 \times 10^{17} \text{ cm}^{-3}$.

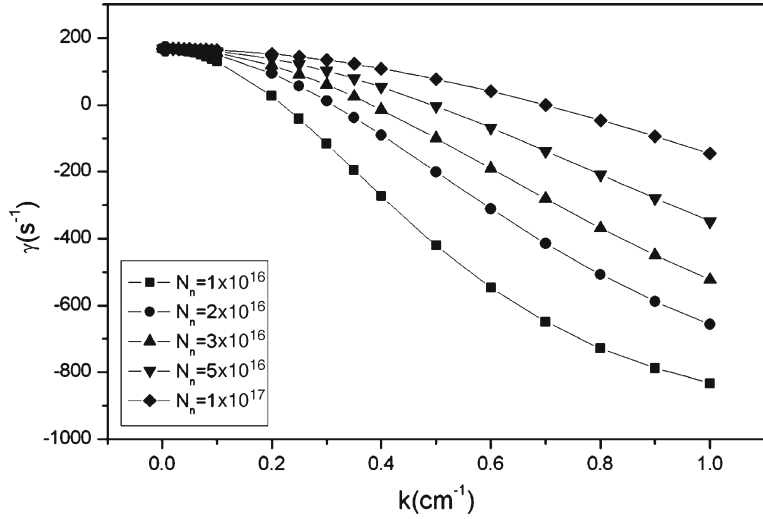


Figure 15. Growth rate γ vs. k , of variable charge with $V_{i0} = 0.005V_{i}$, for different neutral number densities $N_n = 1 \times 10^{16} \text{ cm}^{-3}$, $2 \times 10^{16} \text{ cm}^{-3}$, $3 \times 10^{16} \text{ cm}^{-3}$, $5 \times 10^{16} \text{ cm}^{-3}$, $1 \times 10^{17} \text{ cm}^{-3}$.

parameters [15,23,24]. The recombination frequency is dominant over dust-neutral collision frequency in laboratory plasma as well as in fusion plasma whereas the dust-neutral collision frequency is dominant in the interstellar plasmas.

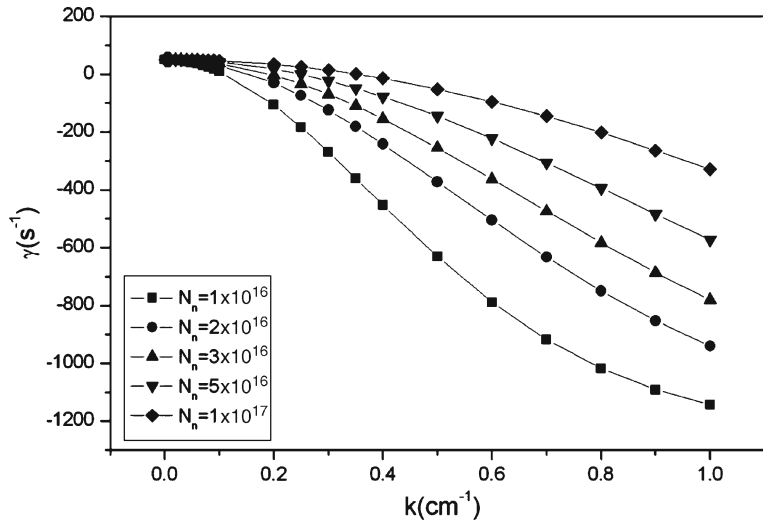


Figure 16. Growth rate γ vs. k , of variable charge with $V_{i0} = 0.01V_{i}$, for different neutral number densities $N_n = 1 \times 10^{16} \text{ cm}^{-3}$, $2 \times 10^{16} \text{ cm}^{-3}$, $3 \times 10^{16} \text{ cm}^{-3}$, $5 \times 10^{16} \text{ cm}^{-3}$, $1 \times 10^{17} \text{ cm}^{-3}$.

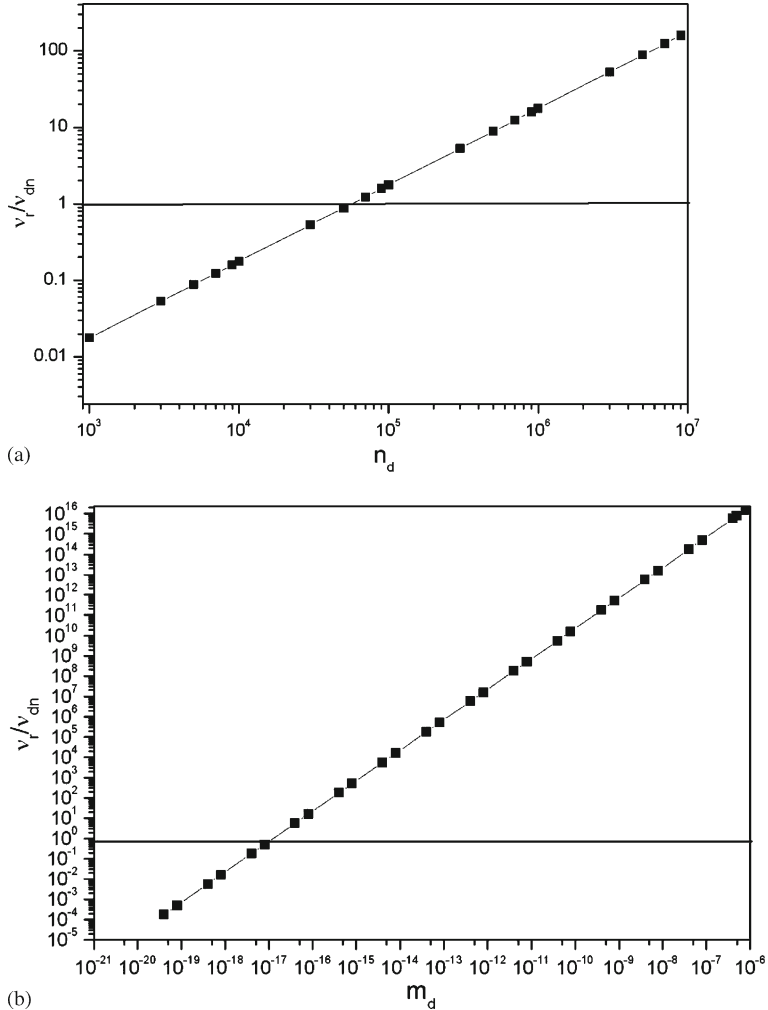


Figure 17. (a) Competition between the effect of recombination (ν_R) and dust-neutral collision frequencies (ν_{dn}) with respect to the dust density. (b) Competition between the effect of recombination (ν_R) and dust-neutral collision frequencies (ν_{dn}) with respect to the dust grain mass.

5. Conclusion

We have investigated the instability of dust-acoustic waves driven by collisions as well as by recombination of electrons and ions on the surface of charged dust grains in dusty plasma with significant pressure of background neutrals. Here we find two distinct regimes, namely short wavelength and long wavelength; the ion-drift and the collisional dust-neutral and ion-neutral momentum transfer drive the short wavelength regime. In long wavelength regime, the recombination effects on the surface of the dust particles

become effective. The effects of neutral densities have also been studied in the presence and absence of ion streaming velocity. Finally, it can be concluded from figures 17a–b that the recombination driven instability is dominant in the long wavelength regime even in the presence of dust-neutral and ion-neutral collisions, while in the shorter wavelength regime, the dust-neutral collision frequency is found to play the dominant role.

In 1997, Kaw and Singh [19] studied the dust-acoustic instability mechanism of dusty plasma where they neglected the dust-neutral collisions with respect to the recombination frequency. Later, Mamun and Shukla [20] reported that dust-neutral frequency is more important than electron–ion recombination on dust driven by instability mechanism. Our investigation reveals that the dust-neutral collision and retardation due to recombination of ions and electrons on the surface of the dust particles both are important but becomes effective for different wavelength regime. The data from the laboratory plasma [16] as well as fusion machines [23] indicate the importance of recombination-dominated collisions over dust collisions, whereas the interstellar plasma [24] data show dominance of dust-neutral collision over the recombination-dominated damping, when dust density less than 10^4 cm^{-3} is considered. We have plotted graph (figures 17a–b) between the ratio of ν_R/ν_{dn} with different dust densities and also with different mass of the dust particles and shown the dominant regime for each damping mechanism. Here, we have found that the recombination is more important than dust-neutral collisions in laboratory plasma [16] and fusion plasma [23], whereas the dust-neutral collision is dominant in the interstellar plasmas [24]. Therefore, we have to be very careful to neglect any one out of the dust-neutral collision and retardation due to the recombination of ions and electrons for the complete description of collisional dusty plasma calculations.

Acknowledgements

We are extremely thankful to Prof. R Singh, IPR for his encouragement and fruitful scientific discussion throughout the course of this paper.

Financial assistance from the Department of Science and Technology, India is gratefully acknowledged.

References

- [1] M Rubel, M Cecconello, J A Malmberg, G Sergienko, W Biel, J R Drake, A Hedqvist, A Huber and V Philipps, *Nucl. Fus.* **41(8)**, 1087 (2001)
- [2] C K Goertz, *Rev. Geophys.* **27**, 271 (1989)
- [3] D B Graves, *IEEE Trans. Plasma Sci.* **22**, 31 (1994)
- [4] H Ikezi, *Phys. Fluids* **29**, 1764 (1986)
- [5] A Barkan *et al*, *Planet Space Sci.* **44**, 239 (1996)
- [6] M Bose, *Plasma Phys. Control Fusion* **37**, 223 (1995)
- [7] N N Rao, P K Shukla and M Y Yu, *Planet. Space Sci.* **38**, 543 (1990)
- [8] P K Shukla and V P Silin, *Phys. Scr.* **45**, 508 (1992)
- [9] J H Chu and I Lin, *Phys. Rev. Lett.* **72**, 4009 (1994)
- [10] H Thomas *et al*, *Phys. Rev. Lett.* **73**, 652 (1994)
- [11] Y Hayashi, *Phys. Rev. Lett.* **83**, 1764 (1994)
Y Hayashi and K Tachibana, *Jpn. J. Appl. Phys.* **33**, L804 (1994)
- [12] M Bose, *Phys. Rev. E* **56(5)**, 5841 (1997)

- [13] F Melandso, *Phys. Plasmas* **3**, 3890 (1996)
- [14] J B Pieper and J Goree, *Phys. Rev. Lett.* **77**, 3137 (1996)
- [15] M Rosenberg, *J. Vac. Sci. Technol. A* **14**, 631 (1996)
- [16] G Prabhuram and J Goree, *Phys. Plasmas* **3**, 1212 (1996)
- [17] N D' Angelo and R L Merlino, *Planet Space Sci.* **12**, 1593 (1996)
- [18] J Goree *et al*, *Phys. Rev. E* **59**, 7055 (1999)
- [19] P K Kaw and R Singh, *Phys. Rev. Lett.* **9**, 423 (1997)
- [20] A A Mamun and P K Shukla, *Phys. Plasmas* **7(11)**, 4412 (2000)
- [21] M Rosenberg, *J. Plasma Phys.* **67**, 235 (2002)
- [22] M R Jana, A Sen and P K Kaw, *Phys. Rev. E* **48**, 3930 (1993)
- [23] S I Krasheninnikov, T K Soboleva, Y Tomita, R D Smirnov and R K Janev, *J. Nucl. Mat.* **337**, 65 (2005)
- [24] R Bharuthram and M Rosenberg, *Planet. Space Sci.* **46(4)**, 425 (1998)